Received: 17 December 2023 | Revised: 20 February 2024 | Accepted: 19 March 2024

DOI: 10.1002/mgg3.2422

Molecular Genetics & Genomic Medicine Open Access WILEY

CLINICAL REPORT

Congenital disorders of glycosylation with multiorgan disruption and immune dysregulation caused by compound heterozygous variants in *MAN2B2*

Shiqi Fan[1] | **Huanhuan Wu**[2] | **Rongrong Wang**[1] | **Qian Chen**[2] | **Xue Zhang**[1]

[1]McKusick-Zhang Center for Genetic Medicine, State Key Laboratory for Complex Severe and Rare Diseases, Institute of Basic Medical Sciences Chinese Academy of Medical Sciences, School of Basic Medicine Peking Union Medical College, Beijing, China

[2]Department of Neurology, The Affiliated Hospital of Capital Institute of Pediatrics, Beijing, China

Correspondence
Xue Zhang, McKusick-Zhang Center for Genetic Medicine, State Key Laboratory for Complex Severe and Rare Diseases, Institute of Basic Medical Sciences Chinese Academy of Medical Sciences, School of Basic Medicine Peking Union Medical College, Beijing, China.
Email: xuezhang@pumc.edu.cn

Qian Chen, Department of Neurology, the affiliated hospital of Capital Institute of Pediatrics, Beijing, China.
Email: chenqianxhl@163.com

Funding information
the National Key Research and Development Program of China, Grant/Award Number: 2022YFC2703900; the CAMS Innovation Fund for Medical Sciences, Grant/Award Number: 2021-1-I2M-018; the National Natural Science Foundation of China, Grant/Award Number: 82394420 and 82394423

Abstract

Background: Congenital disorders of glycosylation (CDG) are a type of inborn error of metabolism (IEM) resulting from defects in glycan synthesis or failed attachment of glycans to proteins or lipids. One rare type of CDG is caused by homozygous or compound heterozygous loss-of-function variants in mannosidase alpha class 2B member 2 (*MAN2B2*). To date, only two cases of *MAN2B2*-CDG have been reported worldwide.

Methods: Trio whole-exome sequencing (Trio-WES) was conducted to screen for candidate variants. N-glycan profiles were measured by liquid chromatography–tandem mass spectrometry (LC–MS/MS). *MAN2B2* expression was evaluated by western blotting. MX dynamin like GTPase 1 (*MX1*) function was estimated via Thogoto virus (THOV) minireplicon assay.

Results: Trio-WES identified compound heterozygous *MAN2B2* (hg19, NM_015274.1) variants (c.384G>T; c.926T>A) in a CDG patient. This patient exhibited metabolic abnormalities, symptoms of digestive tract dysfunction, infection, dehydration, and seizures. Novel immune dysregulation characterized by abnormal lymphocytes and immunoglobulin was observed. The MAN2B2 protein level was not affected, while LC–MS/MS showed obvious disruption of N-glycans and N-linked glycoproteins.

Conclusion: We described a CDG patient with novel phenotypes and disruptive N-glycan profiling caused by compound heterozygous *MAN2B2* variants (c.384G>T; c.926T>A). Our findings broadened both the genetic and clinical spectra of CDG.

KEYWORDS
congenital disorders of glycosylation, inborn error of metabolism, *MAN2B2*, N-glycan

Shiqi Fan and Huanhuan Wu should be considered joint first author.

Xue Zhang and Qian Chen should be considered joint corresponding author.

1 | INTRODUCTION

Congenital disorders of glycosylation (CDG) are a type of inborn error of metabolism (IEM) with high clinical heterogeneity that results from defects in glycan synthesis or failed attachment of glycans to proteins or lipids (Ondruskova et al., 2021). Glycosylation and deglycosylation are two inverse processes involving the addition and trimming of an oligosaccharide chain of varying composition to/from glycoproteins and glycolipids (Ondruskova et al., 2021). *MAN2B2* (OMIM: *618899) encodes a specific α-1,6-mannosidase (EC 3.2.1.24) responsible for the lysosomal glycoprotein degradation to cleave the α-1,6-mannose residue from N-linked glycans (Park et al., 2005), which is vital for recycling free monosaccharides for subsequent glycan synthesis. One rare type of CDG (*MAN2B2*-CDG) is caused by homozygous or compound heterozygous loss-of-function variants in *MAN2B2*. To date, only two cases of *MAN2B2*-CDG have been reported worldwide, one with prominent features of combined immunodeficiency (homozygous variant, c.112G>A, p.Asp38Asn), and another with a typical immune system, cleft palate, and hypospadias (compound heterozygous variants, c.440_442delCTC, p.Ser147del; c.2368G>A, p.Glu790Lys) (Tian et al., 2022; Verheijen et al., 2020). Here, we describe the third *MAN2B2*-CDG patient with metabolic abnormalities, symptoms of digestive tract dysfunction, infection, dehydration, seizures, novel phenotypes of immune dysregulation, and disruptive N-glycan profiling caused by compound heterozygous *MAN2B2* (hg19, NM_015274.1) variants (c.384G>T, p.Gln128His; c.926T>A, p.Ile309Asn).

2 | MATERIALS AND METHODS

2.1 | Ethical compliance

Clinical information and blood samples were collected from the family, and informed consent was obtained. This study was approved by the Peking Union Medical College Institutional Review Board and the Capital Institute of Pediatrics Institutional Review Board in accordance with the Declaration of Helsinki.

2.2 | Trio-WES

Genomic DNA was extracted from the peripheral blood of the patient and healthy parents using a QIAamp DNA Blood Mini Kit (QIAGEN, Cat. No. 51106, Hilden, Germany). DNA libraries were sequenced using an Illumina HiSeq platform with a 100× read depth, and the sequencing data were subsequently mapped to the reference human genome (UCSC GRCh37/hg19) using Burrows–Wheeler Aligner (BWA) software. Functional annotation was performed using ANNOVAR based on public databases, such as dbSNP, 1000 Genomes, gnomAD, and in-house data.

2.3 | Cell culture, plasmid construction and transfection

HEK293T cells were maintained in Dulbecco's modified Eagle medium (Gibco™, Cat. No. C11965500BT, Massachusetts, USA) supplemented with L-glutamine (Gibco™, Cat. No. 25030081), 10% fetal bovine serum (Gibco™, 10,091,148), and penicillin–streptomycin (Gibco™, Cat. No. 15140163) in a 37°C incubator containing 5% CO_2. Transfection was carried out using Lipofectamine™ 3000 reagent (Invitrogen, Cat. No. L3000015, Massachusetts, USA) according to the manufacturer's instructions.

2.4 | Protein extraction

HEK293T cells were washed with phosphate-buffered saline (PBS) (Gibco™, Cat. No. 20012027) and lysed in radioimmunoprecipitation assay (RIPA) buffer (Beyotime, Cat. No. P0013C, Shanghai, China) supplemented with protease inhibitors (Roche, Cat. No. 5892970001, Basel, Switzerland) and phosphatase inhibitors (Roche, Cat. No. 4906837001) while incubating on ice for 30 min. The supernatant was subsequently collected after centrifugation at 14,000 × *g* for 25 min at 4°C.

2.5 | Western blotting

The protein lysate was diluted by adding 4× Protein SDS–PAGE Loading Buffer (TAKARA, Cat. No. 9173, Tokyo, Japan) and RIPA buffer, after which the mixture was boiled at 98°C for 10 min and then incubated on ice for 2 min. Electrophoresis was performed with 7.5% TGX Stain-Free polyacrylamide gels (Bio-Rad, Cat. No. 1610180, California, USA) at 60 V for 45 min followed by 120 V for 120 min. After separation, the protein was transferred to a 0.45 μm Immobilon®-P PVDF Membrane (Millipore, Cat. No. IPVH00010, Massachusetts, USA) at 200 mA for 60 min. Subsequently, the membrane was blocked with 1× Tris-buffered saline–Tween 20 (TBS-T) buffer (Solarbio, Cat. No. T1080) containing 5% skim milk (Solarbio, Cat. No. D8340) at room temperature for 60 min and incubated with primary antibodies diluted in 1× TBS-T on a 4°C rocker overnight. The next day, the membrane was washed with 1× TBS-T four times and then

incubated with horseradish peroxidase-conjugated sheep anti-mouse IgG (ZSGB-Bio, Cat. No. ZB-2305) or sheep anti-rabbit IgG (ZSGB-Bio, Cat. No. ZB-2301, Beijing, China) at room temperature for 60 min. After another four washes with 1× TBS-T, the membranes were exposed to Tanon™ High-sig ECL Western Blotting Substrate (Tanon, Cat. No. 180-5001, Shanghai, China). The primary antibodies used in this study were anti-β-actin (Cell Signaling Technology, CST3700, Massachusetts, USA) and anti-MAN2B2 (Invitrogen, PA5-113537, USA).

2.6 | Thogoto virus (THOV) minireplicon assay

The THOV minireplicon assay was performed as previously described (Mitchell et al., 2012). Briefly, the components of THOV, including PB2, PB1, PA, and NP, were all incorporated into a pCAGGS expression vector. Then, THOV, pHH21-vNP-FF-Luc (firefly luciferase), pRL-TK (renilla luciferase), and MxA plasmids were cotransfected into HEK293T cells using TransIT®-LT1 Transfection Reagent (Mirus, MIR 2304, Madison, USA). A Dual-Luciferase Reporter Assay System (Promega, E1960) was used for the experiment. Twenty-four hours after transfection, luciferase activity was measured on a Synergy H1 reader (BioTek), and the data were presented as the relative luciferase intensity after normalization to Renilla luciferase activity.

2.7 | N-glycan profiling

LC–MS/MS was used for the qualitative and quantitative analyses of N-glycans. Briefly, proteins were extracted from HEK293T cells and quantified, followed by reductive alkylation. Then, the N-glycans were released from the glycoproteins using PNgase F and subsequently enriched, after which the processed samples were analyzed by LC–MS/MS to obtain the raw data. The raw data were subsequently analyzed by Byonic. The structures of the N-glycans were predicted with GlyConnect online tools.

3 | RESULTS

3.1 | Case presentation

3.1.1 | Clinical feature

Our patient was a female infant who was born via spontaneous vaginal delivery at 40^{+3} weeks in a nonconsanguineous family. The weight and height of this patient are 11 kg (P90) and 84 cm (P50), respectively. This patient suffered an ovarian hernia at 1 month of age and underwent high ligation surgery for unilateral inguinal hernia. The patient then presented at 1 year and 2 months with recurrent fever, vomiting, and drowsiness at 1 year and 2 months with repeated fever, frequent vomiting, and severe drowsiness. At that time, the patient vomited more than 10 times a day with no fresh blood or clots in the brown vomit, while her gastric lavage showed bloody substances, which led to mild anemia. In addition, the sleep duration of the patient increased by nearly 5 hours per day compared with the usual duration. Dehydration characterized by poor skin elasticity, low urine volume, dry lips, and few tears when crying were also observed. The preliminary diagnoses of the patient were encephalitis, periodic vomiting, dehydration, metabolic acidosis, mild anemia, and abnormal liver function. These symptoms improved after a period of anti-infection therapy and acidosis correction along with intracranial pressure reduction therapy, however, still recurred once every 1 to 2 months. At the age of 1 year and 8 months, these episodes were further accompanied by convulsions, which were characterized by sudden eye opening followed by gaze, vague consciousness, and motionlessness. Subsequently, left-slanting eyes and rigid shaking of the limbs lasting for a few minutes were observed, seizures occurred several times a day and ended with transient paralysis of the right lower limb at the end of each episode. Therefore, oral antiseizure therapy with oxcarbazepine was added. The intellectual development of this patient was similar to that of her peers during our follow-up period. Notably, according to the self-description from the patient's mother, she had episodes of frequent vomiting beginning at age 6 months, which persisted for approximately 2 to 3 months a year with spontaneous remission and disappeared at age 12. The girl's elder sister was also surgically treated for an ovarian hernia. Overall, this patient exhibited severe multiorgan disruption, especially, symptoms of digestive tract dysfunction, infection, dehydration, and seizures.

3.1.2 | Physical exam

Physical examination of the heart, lungs, and abdomen were all normal. The nervous system showed no positive signs but drowsiness during the episode (photographs of the child were not available).

3.1.3 | Imaging results

The ictal interictal electrocorticogram (EGG) of the patient manifested intermittent, persistent, and diffuse slow

waves predominantly in the left hemisphere (Figure 1a). Brain MRI showed pineal cysts without abnormal signals in the brain parenchyma (Figure 1b). Computed tomography showed that the portal shadow of both lungs was coarse and blurred, suggesting potential lung infection.

3.1.4 | Laboratory results

During the onset of these symptoms, increase in leukocytes with a predominance of neutrophils and markedly elevated C-reactive protein levels were detected in the peripheral blood and cerebrospinal fluid (CSF) of the patient (Table 1). Biochemical tests of the peripheral blood showed elevated aspartate aminotransferase, alanine aminotransferase, fibrinogen equivalent units, and decreased albumin, which all suggested abnormal liver function. Urine metabolite screening revealed ketonuria, blood metabolite screening showed elevated glycine/alanine, decreased leucine/isoleucine, valine/phenylalanine, and carbon dioxide binding capacity, which were considered secondary to ketoacidosis and nutritional disorders. Notably, immune disturbances were also observed in our patient. The proportion of $CD4^+$ T helper (Th) cells in the peripheral blood of our patient was drastically reduced to 9%, and the ratio of $CD8^+$ cytotoxic T (Tc) cells increased to 54%, leading to a severe inversion of the Th/Tc ratio. The percentage of B cells increased to 31%, while the IgG concentration decreased to 3.32 g/L. To sum up, this patient displayed disturbed biochemical indexes and impaired immunity.

3.2 | Compound heterozygous *MAN2B2* variants identified by Trio-WES

Trio-WES was performed using the peripheral blood from the patient and her parents (Figure 2a). Suspected variants meeting the following criteria were retained: (a) minor allele frequency below 1%; (b) located in exon regions or alternative splicing sites; (c) indels, nonsynonymous variants, or synonymous variants probably affecting splicing; (d) predicted to be pathogenic by bioinformatic tools; (e) affected amino acids that are highly conserved across species; and (f) matched the inheritance pattern and patient phenotypes. Compound heterozygous *MAN2B2* variants (NM_015274.1, c.384G>T and c.926T>A) inherited from the heterozygous mother (c.384G>T) and the heterozygous father (c.926T>A) were ultimately identified. Though the *MAN2B2* variants were classified as uncertain significance according to the American College of Medical Genetics and Genomics (ACMG)/Association for Molecular Pathology (AMP) guidelines, both variants were predicted to be damaging by different in silico pathogenicity prediction tools (Table S1), with a CADD score of 26.5 for c.384G>T and 31 for c.926T>A, which were significantly higher than the mutation significance cutoff CADD score for *MAN2B2* (3.313). In addition, neither variant was reported in the gnomAD database, nor the amino acids affected were highly conserved across species (Figure 2b). Therefore, compound heterozygous *MAN2B2* variants were selected as the candidate variant.

Notably, because our patient exhibited immune-related phenotypes, a low-frequency de novo heterozygous *MX1*

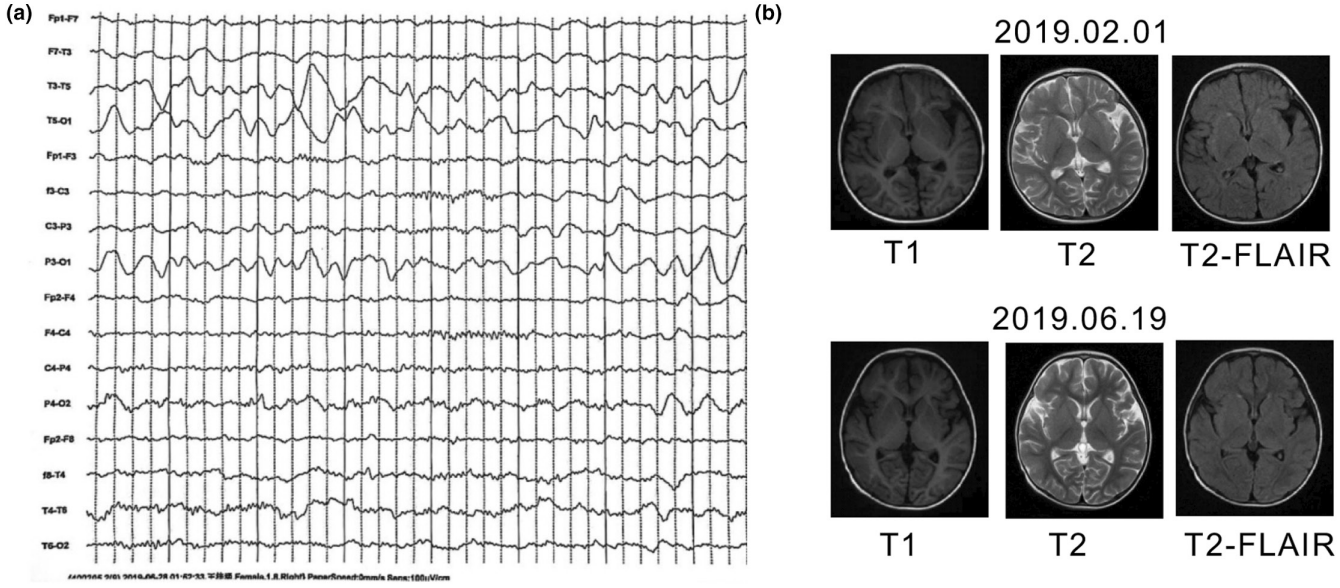

FIGURE 1 EGG and brain magnetic resonance imaging (MRI) of the patient. (a) The EGG of this patient manifested intermittent, persistent, and diffuse slow waves. (b) Brain MRI of the patient. Upper: pineal cysts without abnormal signals in the brain parenchyma; bottom: re-examination of the brain MRI, pineal cysts still existed, and no abnormal signals were found.

TABLE 1 Biochemical test results.

		Time course and patient age					
		2018.12	2019.01	2019.04	2019.05	2019.06	2019.09
Tissue sample	Biochemical tests	1 year and 2 months	1 year and 3 months	1 year and 6 months	1 year and 7 months	1 year and 8 months	1 year and 11 months
Cerebrospinal fluid	Leucocytes ($\times 10^9$/L)	820	20	43	NA	0	NA
	Erythrocyte ($\times 10^9$/L)	NA	440	13,600	NA	0	NA
	Glucose (mmoL/L)	NA	3.34	2.59	NA	2.92	NA
	Total protein (mg/L)	1831	630.5	3405.0	NA	496.9	NA
Peripheral blood	White blood cells ($\times 10^9$/L)	NA	11.98	9.5	7.45	16.16	9.3
	Neutrophil (%)	NA	65.10%	82%	75.70%	84.50%	82.50%
	Hemoglobin (g/L)	NA	103	111	105	106	101
	Platelet ($\times 10^9$/L)	NA	129	129	202	252	272
	C-reactive protein (mg/dL)	NA	41	77	12	83	43

Abbreviation: NA, data not available.

variant (NM_001144925.1, c.1678G>A, p.Asp560Asn) (Figure 4a) was also evaluated, as *MX1* encodes a guanosine triphosphate (GTP)-metabolizing protein responsible for the cellular antiviral response (Haller et al., 2015). The c.1678G>A variant in *MX1* is located in the L4 loop, which is a mutation hotspot domain for recurrent positive selection during primate evolution (Mitchell et al., 2012). The *MX1* variant was predicted to be a tolerated polymorphism by SIFT and MutationTaster, and classified as a variant of uncertain significance according to the ACMG/AMP guidelines. No other suspected variants were associated with immune dysregulation.

3.3 | Disruptive N-glycan profiling caused by compound heterozygous *MAN2B2* variants

Pathogenicity of the compound heterozygous *MAN2B2* variants and the heterozygous *MX1* variant were further estimated. Wild-type *MAN2B2* and the corresponding variant sequences were incorporated into a pcDNA3.1-T2A-EGFP vector, which were subsequently transfected into HEK293T cells. Compared with cells harboring the wild-type *MAN2B2* sequence, MAN2B2 levels in cells transfected with the corresponding compound heterozygous variant sequences remained unchanged (Figure 2c). Given the role of *MAN2B2* in N-linked glycosylation, LC–MS/MS was used to assess the N-glycan profile. HEK293T cells harboring the corresponding *MAN2B2* variant (p.Asp38Asn) identified in the first reported *MAN2B2*-CDG patient (Verheijen et al., 2020) were used as a positive control (Group D). As shown in the Venn diagram in Figure 3a, most of the differentially abundant N-glycans in Group C (transfected with half the c.384G>T variant together with half the c.926T>A variant) compared with Group B (transfected with the wild-type *MAN2B2* sequence) overlapped with those in Group D compared with Group B. These differentially abundant N-glycans also overlapped with those in Group A (transfected with an empty vector) compared with Group B, indicating loss of function of *MAN2B2*. The N-glycans highlighted in red in Figure 3a were displayed in detail in Figure 3b, similar to the *MAN2B2*-CDG patient carrying the homozygous p.Asp38Asn variant (Verheijen et al., 2020), HexNAc(2)Hex(3), HexNAc(2)Hex(4), HexNAc(4)Hex(4), HexNAc(4)Hex(6), and HexNAc(3)Hex(6) were markedly increased, and HexNAc(2) was reduced in Group D when compared with Group B (Figure 3b). Likewise, HexNAc(4)Hex(4), HexNAc(4)Hex(6), and HexNAc(3)Hex(6) were increased, and HexNAc(2) was decreased in Group C (Figure 3b,c). In addition, the differentially abundant N-glycans in Group C exhibited patterns similar to those in another *MAN2B2*-CDG patient harboring the compound heterozygous *MAN2B2* variant (p.Ser147del; p.Glu790Lys) (Tian et al., 2022), which was characterized by accumulation of HexNAc(2)Hex(2) and HexNAc(4)Hex(5) and decrease in HexNAc(2)Hex(7) (Figure 3c). Besides, large-scale dysregulation of other N-glycans was also observed when comparing Group C with Group B (Figure 3d). In conclusion, an overall N-glycosylation disturbance was caused by the *MAN2B2* compound heterozygous variant.

Notably, analysis of the protein–protein interaction (PPI) network of the differentially abundant N-glycoproteins between Group C and Group B revealed that bacterial infection pathways were highly enriched (Figure 3e). In addition, proteins vital to basic biological

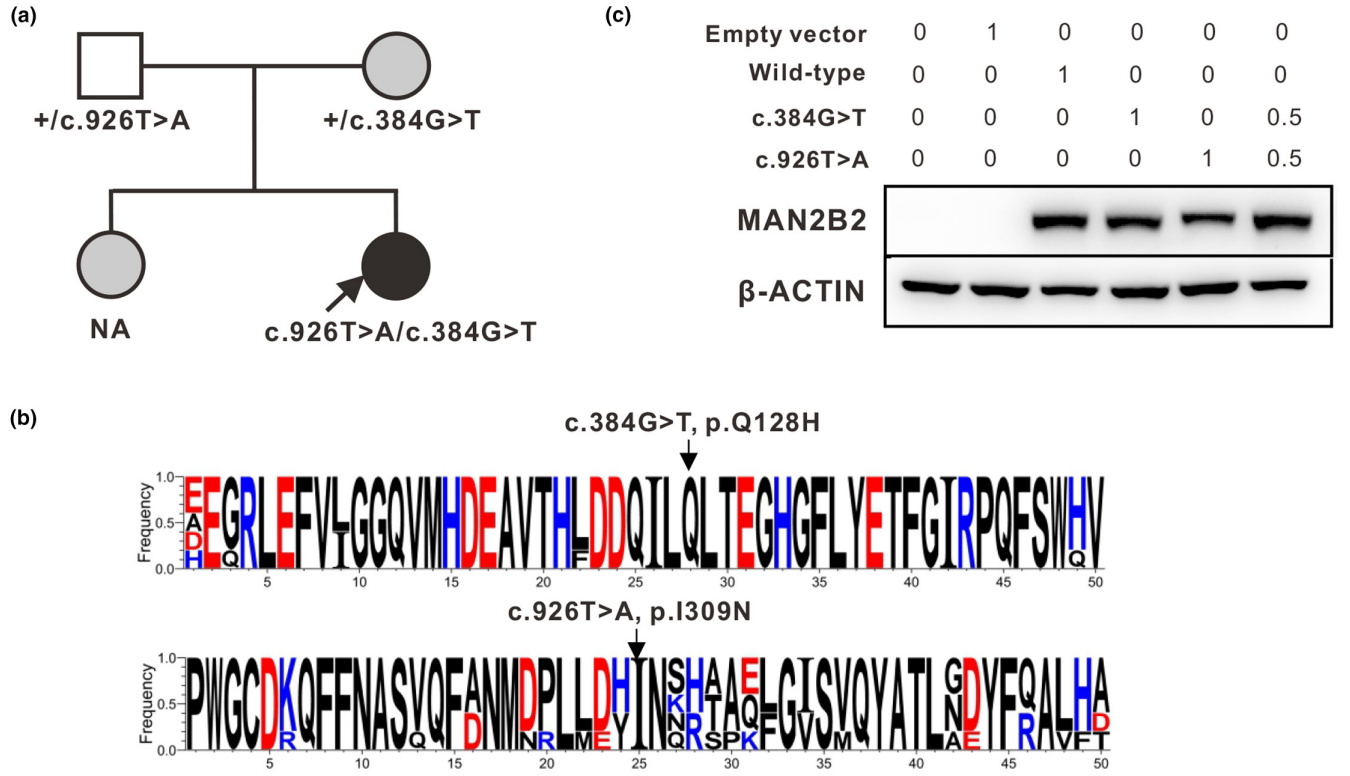

FIGURE 2 Pedigree and expression of the *MAN2B2* variants. (a) Pedigree, the patient suffered multiorgan disruption of CDG (in black), the mother and the patient's elder sister had frequent vomiting and ovarian hernia, respectively (in gray). (b) Amino acid conservation across species. (c) MAN2B2 levels in HEK293T cells transfected with the wild-type *MAN2B2* sequence and/or the *MAN2B2* variant sequence. NA, genetic results not available.

functions such as RNA transport, protein synthesis, cell cycle, apoptosis, and cell junctions were also affected (Figure 3e). The peptides and corresponding proteins modified by altered N-glycans in Group C consistent with those in the *MAN2B2*-CDG patients were listed in Table S2. Notably, the human transcription regulator protein induced by herpes simplex virus infection could interact with SAP30 to inhibit the viral gene transcription (Chen et al., 2010), and therefore, dysregulated N-glycosylation in SAP30BP (SAP30-binding protein) could increase the possibility of virus infection. TOR1AIP1 is a type of integral membrane protein that binds to both lamin A and lamin B to form normal cell structure (Kayman-Kurekci et al., 2014), and TOR1AIP1 dysfunction might lead to the ovarian hernia and unilateral inguinal hernia observed in this patient; and TGFB1 is a pleiotropic factor in the immune system and contributes to various diseases such as immunodeficiency (Kotlarz et al., 2018) and tumors (Trebska-McGowan et al., 2022), dysregulated N-glycosylation of TGFB1 might further worsen immune disturbances. All the differentially abundant N-glycosylated proteins between Group C and Group B are listed in Table S3. In brief, glycoproteins vital for immune system and normal cell function were affected.

The antiviral ability of the *MX1* variant was further assessed using the THOV minireplicon assay as previously reported (Mitchell et al., 2012). HEK293T cells transfected with the c.1678G>A variant showed nearly fourfold reduction in THOV minireplicon ability (Figure 4b), and that in cells transfected with half the wild-type *MX1* sequence and half the c.1678G>A variant sequence was impaired by almost twofold (Figure 4b). The contribution of *MX1* variant to the phenotype could not be excluded

FIGURE 3 N-glycan profiling via LC–MS/MS. (a) Venn diagram. (b) Common differentially abundant N-glycans between Group D compared with Group B and Group C compared with Group B (red highlighted portion in the Venn diagram). (c) Intensity of differentially abundant N-glycans that were consistent with previous reports in the *MAN2B2*-CDG patients. (d) All the differentially abundant N-glycans between Group C and Group B (only |fold change|>5 or <0.2 were displayed). (e) PPI network of the differentially abundant N-glycoproteins between Group C and Group B. Circles denoted proteins, and squares indicated enriched pathways. Group A: transfected with an empty vector; group B: transfected with the wild-type *MAN2B2* sequence; group C: transfected with half the c.384G>T variant together with half the c.926T>A variant; group D: positive control, transfected with the *MAN2B2* variant (p.Asp38Asn).

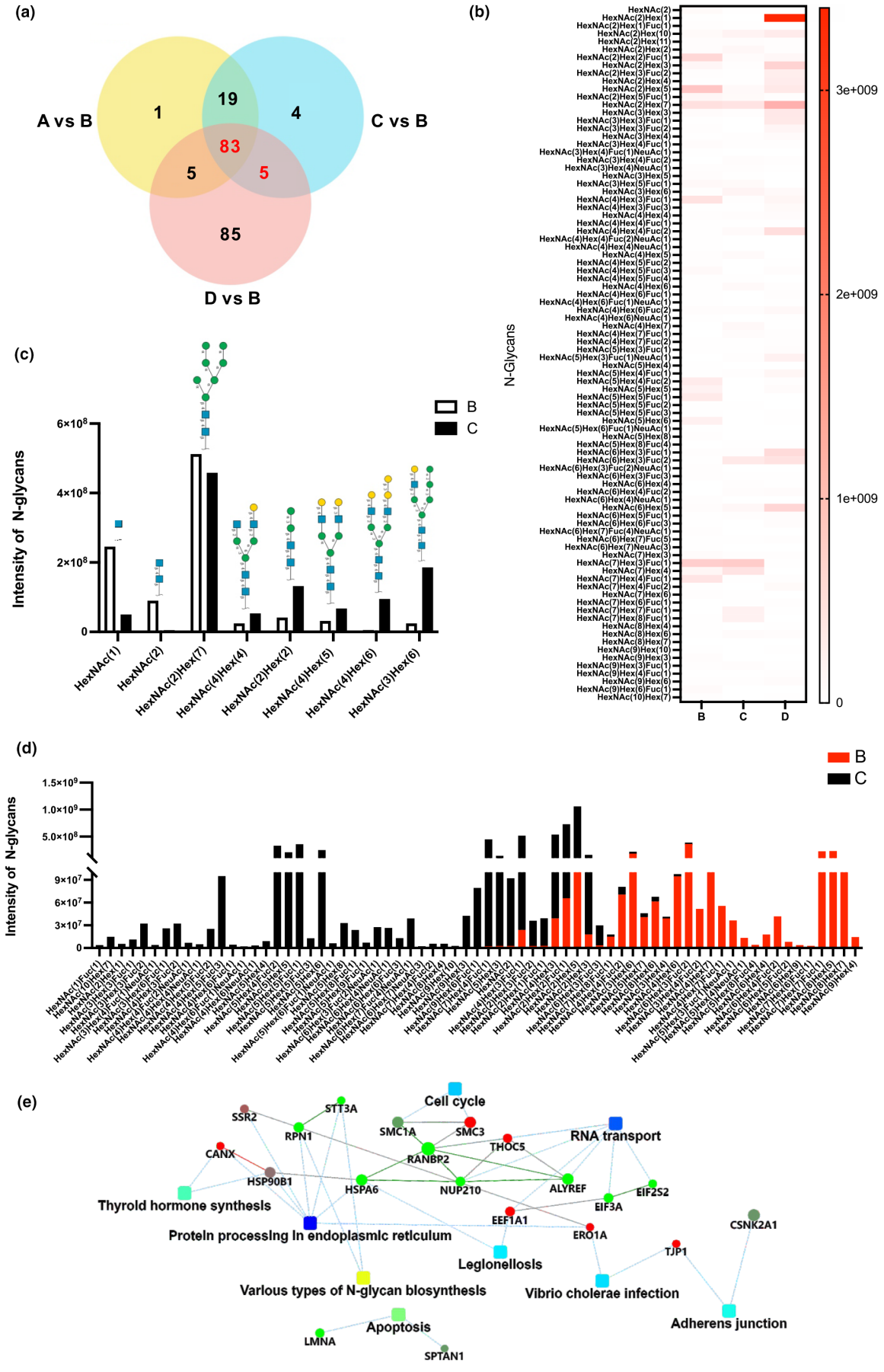
(a)
A vs B
C vs B
D vs B
1
19
4
83
5
5
85
(b)
N-Glycans
3e+009
2e+009
1e+009
0
B
C
D
(c)
Intensity of N-glycans
B
C
6×10^8
4×10^8
2×10^8
0
HexNAc(1)
HexNAc(2)
HexNAc(2)Hex(7)
HexNAc(4)Hex(4)
HexNAc(2)Hex(2)
HexNAc(4)Hex(5)
HexNAc(4)Hex(6)
HexNAc(3)Hex(6)
(d)
Intensity of N-glycans
B
C
1.5×10^9
1.0×10^9
5.0×10^8
9×10^7
6×10^7
3×10^7
0
(e)
Cell cycle
SSR2
STT3A
RPN1
SMC1A
SMC3
THOC5
RNA transport
CANX
RANBP2
HSP90B1
HSPA6
NUP210
ALYREF
EIF2S2
EIF3A
Thyroid hormone synthesis
EEF1A1
ERO1A
CSNK2A1
Protein processing in endoplasmic reticulum
TJP1
Legionellosis
Various types of N-glycan biosynthesis
Vibrio cholerae infection
Adherens junction
Apoptosis
LMNA
SPTAN1

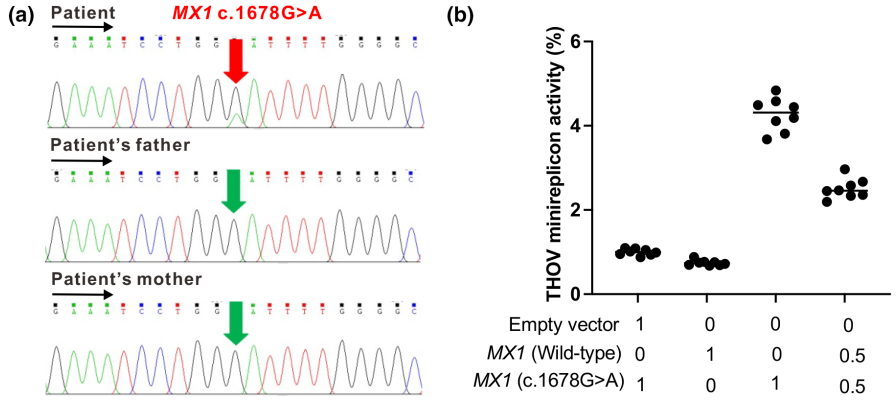

FIGURE 4 Functional evaluation of the *MX1* variant. (a) Sanger sequencing of the *MX1* variant. (b) Anti-THOV activity in HEK293T cells transfected with the wild type*MX1* sequence and/or the *MX1*variant sequence.

though we thought it was less likely due to the following reasons: firstly, the impairment of antiviral ability was not sufficient to cause obvious phenotypes in humans, as the harmful variant caused a nearly one-hundred-fold reduction in THOV minireplicon ability (Mitchell et al., 2012); in addition, direct pathogenicity of the *MX1* variant in human disease has not been determined, and the low Sanger sequencing peak (Figure 4a) indicated that only a small proportion of cells carried this *MX1* variant. Therefore, the immune disturbances in our patient were predominantly caused by the compound heterozygous *MAN2B2* variants.

4 | DISCUSSION

CDG are a series of complex but inseparable disorders with phenotypic overlap among different subtypes. For example, our *MAN2B2*-CDG patient exhibited slight anemia, pneumonia, and gastrointestinal infection, which were consistent with previous reports in *MAN2B1*-deficient patients (Hennermann et al., 2022). Recurrent vomiting/diarrhea was also observed in CDG patients with *MPI* variants (de la Morena-Barrio et al., 2019). In addition, as 1,6-mannose is a core component for the degradation of glycosylphosphatidylinositol (GPI)-anchored proteins, phenotypes of *MAN2B2*-CDG patients might be similar to those of GPI-deficient CDG patients. Therefore, phenotype-based diagnosis is much more difficult and ambiguous than gene-based diagnosis of CDG. Although serum N-glycans, and urinary mannose-rich oligosaccharides are biomarkers for the diagnosis of *MAN2B2*-CDG, genetic testing can not only offer precise diagnosis at the molecular level, but also help to classify disease subtypes (Jones et al., 2013). Thus, further studies of pathogenic *MAN2B2* variants are urgently needed for guiding the clinical diagnosis of CDG. The first case of *MAN2B2*-CDG received hematopoietic stem cell transplantation and rabbit antithymocyte globulin therapy (Verheijen et al., 2020) to improve the immunodeficiency phenotypes. While for our patient, most therapy are symptomatic treatment. Enzyme supplementation might be promising to treat IEM, which needs to be started early and continued. In addition, exogenous hematopoietic stem cell transplantation or genetically modified autologous hematopoietic stem cell transplantation would be for *MAN2B2*-CDG patients with immunodeficiency.

MAN2B2 has nineteen exons in total and is located on chromosome 4. No mutation hotspot domains were observed according to currently available reports. *MAN2B2* was first identified to be expressed in the reproductive tissue (Hiramoto et al., 1997) and was later verified to be ubiquitously expressed throughout the body (Tascou et al., 2000). MAN2B2 belongs to α1,6-mannosidase that is limited to superior species, indicating the complexity of its function. Degradation of the core N-glycans is catalyzed by several glycosidases, including lysosomal α-mannosidase, core-specific α1,6-mannosidase, and β-mannosidase (Park et al., 2005). α-Mannosidosis (OMIM #248500) is a rare autosomal recessive lysosomal storage disorder caused by pathogenic variants in *MAN2B1* (Malm & Nilssen, 2008). *MAN2B2* is believed to play a compensatory role in the degradation of N-glycans by *MAN2B1*; however, three reported *MAN2B2*-CDG cases, including the one described in this study, strongly confirmed that variants in *MAN2B2* alone can cause severe CDG. β-Mannosidosis (OMIM #248510) is another rare autosomal recessive lysosomal storage disorder caused by pathogenic variants in *MANBA* (Sedel et al., 2006), and free glycans processed from MAN2B2 will be degraded by MANBA to finish the last step of glycoprotein degradation. The unique role of *MAN2B2* in deglycosylation process determines that pathogenic variants in *MAN2B2* are sufficient to cause human diseases.

In general, more than 170 types of IEMs are accompanied by immunological manifestations ranging from abnormal immune cell counts, autoimmunity, and autoinflammation to recurrent infections, among which T/B lymphocytes, macrophages, and neutrophils are the most affected cell types in IEMs accompanied by immune

disorders (de Boer et al., 2023). Treatment and management of immune phenotypes are highly important for treating IEMs (Francisco et al., 2020). CDG is a special type of IEM, as they are also classified as inborn errors of immunity (Bousfiha et al., 2022). Different from the immune disturbances observed in the first reported *MAN2B2*-CDG patient (Verheijen et al., 2020), our patient displayed an inversion of the Th/Tc ratio, increased B-cell numbers, decreased IgG contents, and upregulated level of inflammatory markers, which indicated impaired anti-infection ability and a persistent state of inflammation. N-glycosylation is vital for the conformation, expression, stability, and antigenicity of various immunological proteins (Baum & Cobb, 2017). According to the LC–MS/MS results, disruptive N-glycosylation of SAP30 and TGFB1 might be a core element in inducing immune dysregulation of our *MAN2B2*-CDG patients, and other glycoproteins such as TOR1AIP1 vital for normal cell function and biological process were also severely affected, which contribute to multiorgan disturbances. Our *MAN2B2*-CDG case with immune disorders provided new evidence that metabolic defects contribute to immune disturbance, and further studies are needed to elucidate the detailed pathogenic mechanism of IEMs accompanied by immune disturbances.

5 | CONCLUSION

This study described the clinical characteristics and disrupted N-glycan profiles of a CDG patient with compound heterozygous *MAN2B2* variants (NM_015274.1, c.384G>T; c.926T>A). This patient exhibited metabolic abnormalities, symptoms of digestive tract dysfunction, infection, dehydration, seizures, and novel immune phenotypes characterized by an inversion of the Th/Tc ratio, increased B cells, and impaired IgG levels. Disruptive N-glycan profiling and abnormal N-glycosylated proteins caused by *MAN2B2* compound heterozygous variants contributed to the phenotypes. This research advanced our understanding of the genetic spectrum and phenotypic heterogeneity of *MAN2B2*-CDG. Our study also highlighted the importance of genetic testing in CDG diagnosis.

AUTHOR CONTRIBUTIONS

XZ, QC, RW, and SF designed the whole research. Clinical samples and professional medical guidance were provided by QC and HW. SF and HW conducted all the experiments. XZ, QC, and RW supervised the progress. SF prepared the first draft of the manuscript. XZ, RW, QC, and HW independently checked and revised the syntax mistakes and logical errors. All the authors listed contributed to the article.

ACKNOWLEDGEMENTS

We would like to thank all the individuals for their collaboration.

FUNDING INFORMATION

This work was financially supported by the National Key Research and Development Program of China [grant number 2022YFC2703900], the CAMS Innovation Fund for Medical Sciences [grant number 2021-1-I2M-018], and the National Natural Science Foundation of China (grant numbers 82394420 and 82394423).

CONFLICT OF INTEREST STATEMENT

The authors declare no competing interests.

DATA AVAILABILITY STATEMENT

All the datasets were included in the article or supplementary materials, and other data are available from the corresponding author upon request.

ETHICAL APPROVAL

Clinical information and blood samples were collected from the patient and her parents, and the parents (legal guardians) of the child assigned the informed consent on behalf of the child. This study was approved by the Peking Union Medical College Institutional Review Board and the Capital Institute of Pediatrics Institutional Review Board in accordance with the Declaration of Helsinki.

ORCID

Shiqi Fan https://orcid.org/0000-0002-9812-0451
Qian Chen https://orcid.org/0000-0001-9566-9003

REFERENCES

Baum, L. G., & Cobb, B. A. (2017). The direct and indirect effects of glycans on immune function. *Glycobiology*, *27*(7), 619–624. https://doi.org/10.1093/glycob/cwx036

Bousfiha, A., Moundir, A., Tangye, S. G., Picard, C., Jeddane, L., Al-Herz, W., Rundles, C. C., Franco, J. L., Holland, S. M., Klein, C., Morio, T., Oksenhendler, E., Puel, A., Puck, J., Seppänen, M. R. J., Somech, R., Su, H. C., Sullivan, K. E., Torgerson, T. R., & Meyts, I. (2022). The 2022 update of IUIS phenotypical classification for human inborn errors of immunity. *Journal of Clinical Immunology*, *42*(7), 1508–1520. https://doi.org/10.1007/s10875-022-01352-z

Chen, J., Li, Y. M., Li, J. F., Liu, L. D., Liao, Y., Na, R. X., Wang, J. J., Wang, L. C., & Li, Q. H. (2010). Transcriptional regulation by HSV-1 induced HTRP via acetylation system. *Virologica Sinica*, *25*(6), 417–424. https://doi.org/10.1007/s12250-010-3147-8

de Boer, L., Cambi, A., Verhagen, L. M., de Haas, P., van Karnebeek, C. D. M., Blau, N., & Ferreira, C. R. (2023). Clinical and biochemical footprints of inherited metabolic diseases. XII. Immunological Defects. *Molecular Genetics and Metabolism*, *139*(1), 107582. https://doi.org/10.1016/j.ymgme.2023.107582

de la Morena-Barrio, M. E., Wypasek, E., Owczarek, D., Miñano, A., Vicente, V., Corral, J., & Undas, A. (2019). MPI-CDG with transient hypoglycosylation and antithrombin deficiency. *Haematologica*, *104*(2), e79–e82. https://doi.org/10.3324/haematol.2018.211326

Francisco, R., Pascoal, C., Marques-da-Silva, D., Brasil, S., Pimentel-Santos, F. M., Altassan, R., Jaeken, J., Grosso, A. R., Dos Reis Ferreira, V., & Videira, P. A. (2020). New insights into immunological involvement in congenital disorders of glycosylation (CDG) from a people-centric approach. *Journal of Clinical Medicine*, *9*(7), 1–30. https://doi.org/10.3390/jcm9072092

Haller, O., Staeheli, P., Schwemmle, M., & Kochs, G. (2015). Mx GTPases: Dynamin-like antiviral machines of innate immunity. *Trends in Microbiology*, *23*(3), 154–163. https://doi.org/10.1016/j.tim.2014.12.003

Hennermann, J. B., Raebel, E. M., Donà, F., Jacquemont, M. L., Cefalo, G., Ballabeni, A., & Malm, D. (2022). Mortality in patients with alpha-mannosidosis: A review of patients' data and the literature. *Orphanet Journal of Rare Diseases*, *17*(1), 287. https://doi.org/10.1186/s13023-022-02422-6

Hiramoto, S., Tamba, M., Kiuchi, S., Jin, Y. Z., Bannai, S., Sugita, Y., Dacheux, F., Dacheux, J. L., Yoshida, M., & Okamura, N. (1997). Stage-specific expression of a mouse homologue of the porcine 135kDa alpha-D-mannosidase (MAN2B2) in type a spermatogonia. *Biochemical and Biophysical Research Communications*, *241*(2), 439–445. https://doi.org/10.1006/bbrc.1997.7768

Jones, M. A., Rhodenizer, D., da Silva, C., Huff, I. J., Keong, L., Bean, L. J., Coffee, B., Collins, C., Tanner, A. K., He, M., & Hegde, M. R. (2013). Molecular diagnostic testing for congenital disorders of glycosylation (CDG): Detection rate for single gene testing and next generation sequencing panel testing. *Molecular Genetics and Metabolism*, *110*(1–2), 78–85. https://doi.org/10.1016/j.ymgme.2013.05.012

Kayman-Kurekci, G., Talim, B., Korkusuz, P., Sayar, N., Sarioglu, T., Oncel, I., Sharafi, P., Gundesli, H., Balci-Hayta, B., Purali, N., Serdaroglu-Oflazer, P., Topaloglu, H., & Dincer, P. (2014). Mutation in TOR1AIP1 encoding LAP1B in a form of muscular dystrophy: A novel gene related to nuclear envelopathies. *Neuromuscular Disorders*, *24*(7), 624–633. https://doi.org/10.1016/j.nmd.2014.04.007

Kotlarz, D., Marquardt, B., Barøy, T., Lee, W. S., Konnikova, L., Hollizeck, S., Magg, T., Lehle, A. S., Walz, C., Borggraefe, I., Hauck, F., Bufler, P., Conca, R., Wall, S. M., Schumacher, E. M., Misceo, D., Frengen, E., Bentsen, B. S., Uhlig, H. H., … Klein, C. (2018). Human TGF-β1 deficiency causes severe inflammatory bowel disease and encephalopathy. *Nature Genetics*, *50*(3), 344–348. https://doi.org/10.1038/s41588-018-0063-6

Malm, D., & Nilssen, Ø. (2008). Alpha-mannosidosis. *Orphanet Journal of Rare Diseases*, *3*, 21. https://doi.org/10.1186/1750-1172-3-21

Mitchell, P. S., Patzina, C., Emerman, M., Haller, O., Malik, H. S., & Kochs, G. (2012). Evolution-guided identification of antiviral specificity determinants in the broadly acting interferon-induced innate immunity factor MxA. *Cell Host & Microbe*, *12*(4), 598–604. https://doi.org/10.1016/j.chom.2012.09.005

Ondruskova, N., Cechova, A., Hansikova, H., Honzik, T., & Jaeken, J. (2021). Congenital disorders of glycosylation: Still "hot" in 2020. *Biochimica et Biophysica Acta - General Subjects*, *1865*(1), 129751. https://doi.org/10.1016/j.bbagen.2020.129751

Park, C., Meng, L., Stanton, L. H., Collins, R. E., Mast, S. W., Yi, X., Strachan, H., & Moremen, K. W. (2005). Characterization of a human core-specific lysosomal {alpha}1,6-mannosidase involved in N-glycan catabolism. *The Journal of Biological Chemistry*, *280*(44), 37204–37216. https://doi.org/10.1074/jbc.M508930200

Sedel, F., Friderici, K., Nummy, K., Caillaud, C., Chabli, A., Dürr, A., Lubetzki, C., & Agid, Y. (2006). Atypical Gilles de la Tourette syndrome with beta-mannosidase deficiency. *Archives of Neurology*, *63*(1), 129–131. https://doi.org/10.1001/archneur.63.1.129

Tascou, S., Nayernia, K., Engel, W., & Burfeind, P. (2000). Refinement of the expression pattern of a mouse homologue of the porcine 135-kDa alpha-d-mannosidase (MAN2B2). *Biochemical and Biophysical Research Communications*, *272*(3), 951–952. https://doi.org/10.1006/bbrc.2000.2868

Tian, Q., Shu, L., Shu, C., Xi, H., Ma, N., Mao, X., & Wang, H. (2022). Compound heterozygous variants in MAN2B2 identified in a Chinese child with congenital disorders of glycosylation. *European Journal of Human Genetics*, *31*, 1455–1457. https://doi.org/10.1038/s41431-022-01125-7

Trebska-McGowan, K., Chaib, M., Alvarez, M. A., Kansal, R., Pingili, A. K., Shibata, D., Makowski, L., & Glazer, E. S. (2022). TGF-β alters the proportion of infiltrating immune cells in a pancreatic ductal adenocarcinoma. *Journal of Gastrointestinal Surgery*, *26*(1), 113–121. https://doi.org/10.1007/s11605-021-05087-x

Verheijen, J., Wong, S. Y., Rowe, J. H., Raymond, K., Stoddard, J., Delmonte, O. M., Bosticardo, M., Dobbs, K., Niemela, J., Calzoni, E., Pai, S. Y., Choi, U., Yamazaki, Y., Comeau, A. M., Janssen, E., Henderson, L., Hazen, M., Berry, G., Rosenzweig, S. D., … Morava, E. (2020). Defining a new immune deficiency syndrome: MAN2B2-CDG. *The Journal of Allergy and Clinical Immunology*, *145*(3), 1008–1011. https://doi.org/10.1016/j.jaci.2019.11.016

SUPPORTING INFORMATION

Additional supporting information can be found online in the Supporting Information section at the end of this article.

How to cite this article: Fan, S., Wu, H., Wang, R., Chen, Q., & Zhang, X. (2024). Congenital disorders of glycosylation with multiorgan disruption and immune dysregulation caused by compound heterozygous variants in *MAN2B2*. *Molecular Genetics & Genomic Medicine*, *12*, e2422. https://doi.org/10.1002/mgg3.2422